MOLECULAR ECOLOGY

Molecular Ecology (2015) **24**, 3964–3979 doi: 10.1111/mec.13284

Geographic and temporal dynamics of a global radiation and diversification in the killer whale

PHILLIP A. MORIN,* KIM M. PARSONS,† FREDERICK I. ARCHER,* MARÍA C. ÁVILA-ARCOS,‡ LANCE G. BARRETT-LENNARD,§ LUCIANO DALLA ROSA,¶ SEBASTIÁN DUCHÊNE,** JOHN W. DURBAN,*† GRAEME M. ELLIS,†† STEVEN H. FERGUSON,‡‡ JOHN K. FORD,†† MICHAEL J. FORD,§§ CRISTINA GARILAO,¶¶ M. THOMAS P. GILBERT,‡*** KRISTIN KASCHNER,††† CRAIG O. MATKIN,‡‡‡ STEPHEN D. PETERSEN,§§§ KELLY M. ROBERTSON,* INGRID N. VISSER,¶¶¶ PAUL R. WADE,† SIMON Y. W. HO** and ANDREW D. FOOTE‡****

*Southwest Fisheries Science Center, National Marine Fisheries Service, NOAA, 8901 La Jolla Shores Dr., La Jolla, CA 92037, USA, †Alaska Fisheries Science Center, National Marine Fisheries Service, NOAA, 7600 Sand Point Way NE, Seattle, WA 98115, USA, ‡Centre for GeoGenetics, Natural History Museum of Denmark, University of Copenhagen, Øster Voldgade 5-7, 1350 Copenhagen, Denmark, §Vancouver Aquarium Marine Science Centre, 845 Avison Way, Vancouver, British Columbia V6G 3E2, Canada, ¶Laboratório de Ecologia e Conservação da Megafauna Marinha, Instituto de Oceanografia, Universidade Federal do Rio Grande, Av. Itália km. 8 s/n, Campus Carreiros, Rio Grande, RS 96201-900, Brazil, **School of Biological Sciences, University of Sydney, Sydney, NSW 2006, Australia, ††Fisheries and Oceans Canada, Pacific Biological Station, 3190 Hammond Bay Rd, Nanaimo, British Columbia, Canada, ‡‡Fisheries & Oceans Canada, 501 University Crescent, Winnipeg, Manitoba R3T 2N6, Canada, §§Northwest Fisheries Science Center, National Marine Fisheries Service, NOAA 2725 Montlake Blvd E, Seattle, WA, USA, ¶¶GEOMAR Helmholtz-Zentrum für Ozeanforschung Kiel Düsternbrooker Weg 2, 24105 Kiel, Germany, ***Trace and Environmental DNA laboratory, Department of Environment and Agriculture, Curtin University, Perth, Western Australia 6845, Australia, †††Department of Biometry and Environmental System Analysis, Albert-Ludwigs-University of Freiburg, Tennenbacher Strasse 4, 79106 Freiburg, Germany, ‡‡‡North Gulf Oceanic Society, 3430 Main St. Ste. B1, Homer, AK 99603, USA, §§§Assiniboine Park Zoo, 2595 Roblin Blvd, Winnipeg, Manitoba R3P 2N7, Canada, ¶¶¶Orca Research Trust, P.O. Box 402043, Tutukaka, Northland 0153, New Zealand, ****Department of Evolutionary Biology, Evolutionary Biology Centre, Uppsala University, Norbyvägen 18D, SE-752 36 Uppsala, Sweden*

Abstract

Global climate change during the Late Pleistocene periodically encroached and then released habitat during the glacial cycles, causing range expansions and contractions in some species. These dynamics have played a major role in geographic radiations, diversification and speciation. We investigate these dynamics in the most widely distributed of marine mammals, the killer whale (*Orcinus orca*), using a global data set of over 450 samples. This marine top predator inhabits coastal and pelagic ecosystems ranging from the ice edge to the tropics, often exhibiting ecological, behavioural and morphological variation suggestive of local adaptation accompanied by reproductive isolation. Results suggest a rapid global radiation occurred over the last 350 000 years. Based on habitat models, we estimated there was only a 15% global contraction of core suitable habitat during the last glacial maximum, and the resources appeared to sustain a constant global effective female population size throughout the Late Pleistocene. Reconstruction of the ancestral phylogeography highlighted the high mobility of this species, identifying 22 strongly supported long-range dispersal events including inter-oceanic and interhemispheric movement. Despite this propensity for geographic dispersal, the increased sampling of this study uncovered very few potential examples of ancestral dispersal among ecotypes. Concordance of nuclear and mitochondrial data further confirms genetic cohesiveness, with little or no current gene flow among sympatric ecotypes. Taken as a whole, our data suggest that the glacial cycles influenced

Correspondence: Phillip A. Morin, Fax: 619-546-7003;
E-mail: phillip.morin@noaa.gov

local populations in different ways, with no clear global pattern, but with secondary contact among lineages following long-range dispersal as a potential mechanism driving ecological diversification.

Keywords: cetacean, habitat models, mitogenomics, phylogeography, single nucleotide polymorphism, speciation

Received 3 March 2014; revision received 9 June 2015; accepted 17 June 2015

Introduction

The glacial cycles of the quaternary are thought to have had a large effect on ancestral distribution, demography and connectivity and ultimately to have shaped the genetic make-up of extant populations (Hewitt 2000; Blois *et al.* 2010; Hofreiter & Barnes 2010; Lorenzen *et al.* 2011). Outcomes of these dynamics can include rapid range shifts, local adaptation and speciation (Hewitt 1996; Lovette 2005; Carstens & Knowles 2007). For example, marine threespine sticklebacks (*Gasterosteus aculeatus*) have colonized freshwater systems throughout the species range; at high latitudes, this occurred following the retreat of the ice sheets after the last glacial maximum (LGM), and in some lakes, a second post-glacial invasion has led to further diversification of limnetic and benthic freshwater forms (McKinnon & Rundle 2002). Similarly, the rich diversity of cichlid species in some of the African great lakes, such as Lake Victoria, have arisen since the great droughts of the Late Pleistocene, ~15 000 years ago in the case of Lake Victoria (Sturmbauer *et al.* 2001; Wagner *et al.* 2013). Climate change during the Late Pleistocene is even thought to have played a role in the spread of modern humans out of Africa (Carto *et al.* 2009; Muller *et al.* 2011). Less is known about how glacial cycles influenced the historical connectivity and demography of marine mammal populations (O'Corry-Crowe 2008). For some marine mammal species, genetic data suggest demography and connectivity between populations has changed concurrent with the glacial cycles (Pastene *et al.* 2007; Alter *et al.* 2012, 2015; Amaral *et al.* 2012; Foote *et al.* 2013a). The killer whale (*O. orca*) is a globally distributed species for which the role of climatic change upon demography and connectivity has become highly debated, and is therefore emerging as a potentially useful study organism for reconstructing the ancestral population history to better understand the demographic impacts of the glacial cycles.

Killer whales are found in all oceans of the world, though their densities are typically highest in productive coastal regions and at higher latitudes (Forney & Wade 2006). Although killer whales are still recognized as a single species globally, studies focusing on three geographic regions have demonstrated a range of dietary specializations among groups that is generally associated with morphological, behavioural and ecological differences. Observations of multiple sympatric ecotypes or morphotypes in several regions have generated a significant amount of research on social structure, niche specialization, population structure, and patterns and modes of speciation (e.g. Bigg *et al.* 1990; Ford *et al.* 1998, 2000, 2011; Pitman & Ensor 2003; Hoelzel *et al.* 2007; Foote *et al.* 2009, 2011b, 2013c; Morin *et al.* 2010; Moura *et al.* 2014b, 2015). However, there is still much debate regarding the mechanisms and processes driving this evolutionary diversification. These unresolved debates include the mode of phylogeographic diversification, and in particular whether sympatric ecotypes evolved in situ or in allopatry, followed by secondary contact (Foote *et al.* 2011b; Foote & Morin 2015; Moura *et al.* 2015); and the degree to which the mitochondrial phylogeny reflects either a stochastic distribution of lineages following a global bottleneck (Hoelzel *et al.* 2002; Moura *et al.* 2014a), or a highly sorted tree consistent with ecotypes potentially representing incipient species (Morin *et al.* 2010). All of these studies have been limited by incomplete taxon sampling, which may present a major bias (see Foote & Morin 2015), particularly in phylogeographic analyses that depend upon the inference of ancestral distributions (e.g. Foote *et al.* 2011b; Moura *et al.* 2015).

To better understand the geographic context and evolutionary processes that gave rise to the present-day global diversity of killer whales, we conducted population genomic and phylogeographic analyses of the most geographically and ecologically diverse sample of killer whales to date and modelled the global distribution of core suitable habitat based on paleo-climate data from the last glacial maximum (LGM) and present-day climatic conditions. Specifically, our aims were (1) to better understand the geographic context and origins of ecological diversification through increased sampling across the known range, (2) to better understand the timing and tempo of diversification and its relationship to demography and changes in the distribution and extent of suitable habitat and (3) to re-evaluate the support for genetically independent ecotypes or populations from maternally inherited mitochondrial genomes and from biparentally inherited nuclear markers.

Materials and methods

Samples and DNA sequencing

To increase the scope of this study beyond that of previous studies, which mainly consisted of samples collected through dedicated research at known high-density regions, we conducted a broad search for samples collected by marine mammal researchers globally. The resulting contributions of samples include those collected more opportunistically to include low-density regions and better sampling across the species' range (Fig. 1). Additional sampling within known ecotypes (residents, transients, Antarctic types B, C) were

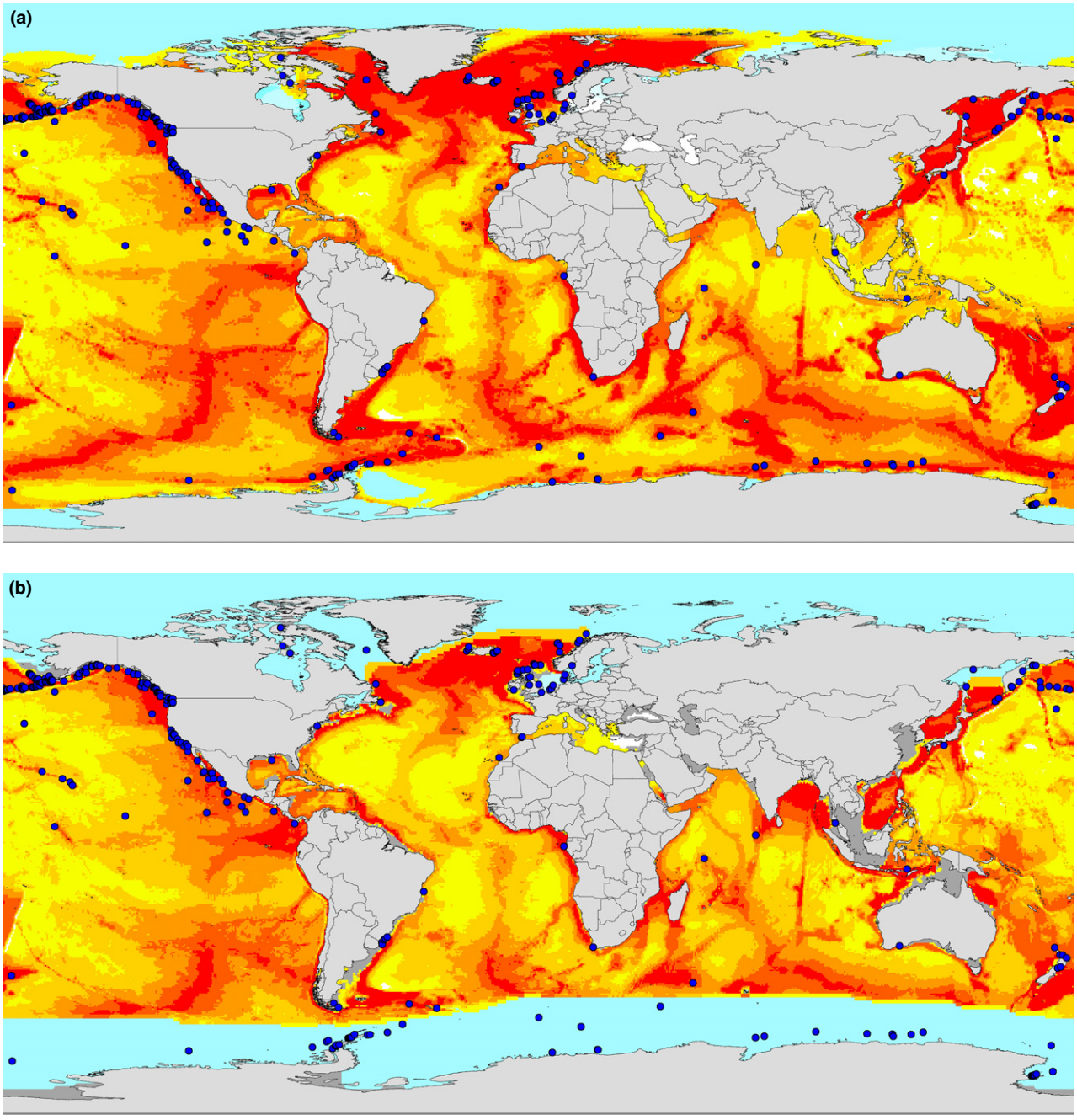

Fig. 1 Map showing origin of samples used in this study overlain on the AquaMaps suitable habitat map for killer whales of the (a) present day and (b) the last glacial maximum (LGM). Yellow to red colours represent least to most suitable habitat, respectively, based on the AquaMaps habitat model (see Materials and methods). Light blue colour represents areas with >50% sea ice concentration during both time periods. Land exposed due to sea level changes during the LGM is shown in dark grey.

selected to maximize the number of social groups sampled (one per group) and geographic distribution. Detailed sample information and DNA extraction information is in Table S1 (Supporting information).

Mitogenome sequences were combined from previous publications ($N = 169$) and newly generated data ($N = 283$ excluding replicates; see Results). A subset ($n = 36$) of the samples was sequenced at the Centre for GeoGenetics, Natural History Museum of Denmark, using methods describe in Foote *et al.* (2013b,c). The remaining 247 samples were sequenced at the Southwest Fisheries Science Center using multiplexed DNA libraries for capture enrichment and next-generation sequencing of both mitochondrial and nuclear loci. Indexed DNA libraries were prepared and pooled according to methods described by Hancock-Hanser *et al.* (2013) with minor changes as follows. Each pooled indexed library was divided into two portions for separate capture enrichment of the mitogenome and the nuclear loci. The amount of DNA in each portion varied by library pool, with a minimum of 100–200 ng used for mtDNA enrichment, and 300–800 ng used for nuclear enrichment from modern tissue samples. Libraries prepared from historical tooth samples used all DNA available from a single extraction (see Morin *et al.* 2006 for extraction methods), and DNA was not sonicated prior to ligation. Two SureSelect DNA capture arrays were designed as previously described (Hancock-Hanser *et al.* 2013). One included one copy of probes spaced every 15 bp across the killer whale mitogenome (Accession no. GU187193.1) and nine copies of probes every 3 bp across 78 nuclear loci described by Hancock-Hanser *et al.* (2013) from the common bottlenose dolphin (*Tursiops truncatus*) genome (assembly turTru1, Jul 2008; database version 69.1; Flicek *et al.* 2013; Lindblad-Toh *et al.* 2011). The second contained only nine copies of the probes for the 78 nuclear loci (Table S2, Supporting information). After capture enrichment, libraries were amplified and sequenced in separate lanes using single-end 100 bp sequencing on an Illumina HiSeq2000 Analyzer.

Mitogenome assembly

Assembly of reads to the reference mitogenome or nuclear sequences was performed using custom R scripts and publicly available programs as previously described (Hancock-Hanser *et al.* 2013; Dryad data repository doi: 10.5061/dryad.cv35b). The reference mitochondrial sequence (Accession no GU187164) was modified to improve assembly coverage at the 'ends' of the linearized mitogenome by adding 40 bp from each end to the opposite end (so that reads could map across the artificial break point of the linearized sequence). All sequences were aligned and visually inspected in the program GENEIOUS (V. 6.0.5, Biomatters, Auckland, New Zealand), and indels and unique variants were verified in the BAM files.

Nuclear locus assembly, SNP discovery and SNP genotyping

As bottlenose dolphin sequences had been used for DNA library enrichment and are expected to differ from the killer whale sequences (thereby reducing assembly efficiency for SNP discovery and genotyping), consensus killer whale sequences were generated in a two-step process. First, ten samples with high read counts were combined and mapped to the bottlenose dolphin reference sequences used for library enrichment in CLC GENOMICS WORKBENCH (v. 4.9, CLC bio, Cambridge, MA, USA). The 78 loci were covered at an average depth of 230 reads (range 94 to 653 982). Second, to maximize the length of the nuclear loci, potentially capturing sequence beyond the ends of the reference sequences, five samples with very high numbers of reads were selected (each with 1.9–4.7 million reads) and combined for de novo assembly in CLC GENOMICS WORKBENCH. The resulting 429 contigs (minimum size = 500 bp) were imported into GENEIOUS and assembled to the previously generated killer whale reference sequences (above). Consensus sequences that maximized the length of each locus were saved as the new reference sequences (Accession no. KR014267–KR014 271; Table S2, Supporting information) for assembly and SNP discovery from individual samples.

SNPs were chosen from a panel of 114 globally distributed samples selected for geographic and ecotypic diversity and good average depth of coverage across the nuclear loci. Detailed methods for SNP validation and genotyping from NGS data are provided in Table S3 (Supporting information). Analysis of deviations from expectations of Hardy–Weinberg equilibrium (HWE) and linkage disequilibrium (LD) were calculated using GENEPOP (v. 4.2; Raymond & Rousset 1995) in five strata containing >15 samples (Table S3, Supporting information). Jackknife analyses to detect genotypes that affected divergence from expectations of HWE were conducted as described in Morin *et al.* (2009). We used the program STRUCTURE to analyse all SNPs to identify strongly supported groups and to assign some samples to groups for the purpose of pairwise population differentiation analyses (Fig. S1, Supporting information).

For a priori population differentiation tests (F_{ST}), populations were based primarily on individuals assigned to ecotype/morphotype in the field, or assigned to geographically disjunct groups. A few individuals were assigned to populations solely based on genetic

evidence, or on a combination of genetics and morphology (e.g. a type C whale that stranded in Brazil). SNPs found within the same contig (typically <1200 bp) were assumed to be linked and combined into haplotypes using the program PHASE (Stephens *et al.* 2001), using 5000 iterations and haplotype probability cut-off of 0.5 for inferred haplotypes, and samples stratified by populations (Table S4, Supporting information). This resulted in a set of 42 loci, 25 of which consisted of phased multi-SNP genotypes. We also selected a single SNP from each of the 25 loci that contained multiple SNPs to analyse only unlinked bi-allelic SNPs (42 unlinked SNPs). From each multi-SNP locus, we selected the SNP with the highest expected heterozygosity in the full data set (H_{exp}, Table S3, Supporting information). A full listing of samples in each stratum used for PHASE, STRUCTURE and a priori population differentiation analyses is provided in Table S4 (Supporting information).

Tajima's *D* (Tajima 1989) and Fay and Wu's *H* (Fay & Wu 2000) were calculated using DNASP (v. 5.10.1, Librado & Rozas 2009) for all samples and for four clades that correspond to known ecotypes or geographic populations (Northeast Atlantic, Antarctic C, residents, transients).

Phylogenetic analyses

To estimate the evolutionary and demographic timescale of the killer whale phylogeny, we employed a two-step approach. In the first step, we obtained published mitogenomic sequences from 17 delphinids (Table S5, Supporting information). We added two of the most divergent killer whale sequences (MtGen_94 from Clade 12 and MtGen_106 from Clade 1) to capture the most recent common ancestor of the sampled individuals. We used the Bayesian phylogenetic approach implemented in BEAST v1.8.1 (Drummond *et al.* 2012) to estimate the tree topology and divergence times. This analysis was based on the 13 protein-coding genes and 2 rRNA genes, with the optimal partitioning scheme for the substitution models selected using PartitionFinder (Lanfear *et al.* 2012). The optimal scheme involved partitioning the genes into four subsets (Table S6, Supporting information), with an independent substitution model assigned to each group of genes. We used a Yule prior for the tree, with an uncorrelated lognormal relaxed clock to account for rate variation among lineages (Drummond *et al.* 2006). The clock was calibrated using a normal prior (mean 10.08 Myr, standard deviation 1.413 Myr) for the age of the root node (McGowen *et al.* 2009). Posterior distributions of parameters were estimated using Markov chain Monte Carlo (MCMC) simulation, with samples drawn every 10^3 steps over a total of 10^7 steps. The first 10% of samples were discarded as burn-in, with the remaining samples checked for acceptable convergence and mixing (all ESS > 200).

In the second step of our molecular dating analysis, we performed a Bayesian coalescent analysis of 158 mitogenome haplotypes from killer whales. To minimize the impact of incomplete purifying selection, which can lead to overestimation of the substitution rate on short timescales (Ho *et al.* 2011), we only used the third codon sites of the 13 protein-coding genes. We used PartitionFinder to identify the optimal partitioning scheme, which involved dividing the genes into two subsets (Table S6, Supporting information). Using Bayes factors, we found decisive support for a constant-size coalescent prior compared with the more flexible Bayesian skyride model, both for all haplotypes and for all samples in well-sampled groups representing known ecotypes or populations (resident, transient, Antarctic type C, N. Atlantic herring feeders). BEAST input files and the maximum-clade-credibility tree file are available from the Dryad repository (doi: 10.5061/dryad.fm4mk).

To investigate and infer biogeographical patterns and processes, we applied the Bayesian Binary MCMC method (BBM) implemented in the RASP (Reconstruct Ancestral State in Phylogenies) 3.02 software package (Yu *et al.* 2014). This method reconstructs ancestral character states at given nodes, along with the transformations between these states, using Bayesian inference to account for the uncertainty in both the phylogenetic tree and the mapping of character state (see Ronquist 2004). The global distribution of killer whales was divided into seven areas: North Pacific, Tropical Pacific, South Pacific, North Atlantic, South Atlantic, Southern Ocean and Indian Ocean. Each tip of the mitogenome tree was assigned to one of these areas. We allowed a maximum of four areas to be inferred as the ancestral distribution at each node. The MCMC analysis was run using 10 chains, with a temperature parameter of 0.5. Samples were drawn every 100 MCMC cycles over a total of 10^6 cycles, with the first 10^5 cycles discarded as burn-in. We restricted our analysis to nodes with a posterior probability of ≥90%.

SNAPP (v. 1.1.1, Bryant *et al.* 2012) was used to infer multilocus phylogenetic trees from nuclear SNPs based on the coalescent. SNAPP assumes independent bi-allelic SNPs, so we used the 42 single SNPs described above and included only samples (N = 113) from the 12 populations represented by at least three samples. We used the default prior and model parameters and ran a single MCMC chain of 500 000 iterations with sampling every 1000 steps. Acceptable mixing and convergence were checked by visual inspection of the posterior samples. We used a burn-in of 10% and visualized the distribution of trees using DENSITREE (v. 2.1, Bouckaert

2010). The maximum-clade-credibility tree was generated using TREEANNOTATOR (v. 1.7.4, Drummond & Rambaut 2007). The SNAPP input file and trees are available from the Dryad repository (doi: 10.5061/dryad.fm4mk).

Support for populations and ecotypes by nuclear SNPs

To test hypotheses of divergence between putative populations and ecotypes, the pairwise divergence metric F_{ST} (Wright 1931; Weir & Cockerham 1984) was calculated using the R package 'strataG' (R Development Core Team 2011). For all analyses, 1000 permutations were used to calculate the *P*-value.

Habitat suitability model

We used the AquaMaps approach (Ready *et al.* 2010; Kaschner *et al.* 2011; www.aquamaps.org) to species distribution modelling for mapping the distribution of suitable habitat for killer whales at the present and during the last glacial maximum (LGM; ~20 000 calendar years before present). In contrast to other existing species distribution models, AquaMaps was developed specifically to deal with prevailing nonrepresentative sampling of large-scale marine species ranges and the overall paucity of available point-occurrence records. By allowing for the incorporation of expert knowledge about species-specific habitat usage as input into the model, the AquaMaps approach attempts to account for some of the known biases that can be attributed to skewed effort distributions and potential errors in species identifications. In this context, habitat usage of species can be described based on a predefined set of environmental parameters including depth, temperature, salinity, primary production and sea ice concentration. This is subsequently projected into geographic space in a global grid of 0.5° latitude by 0.5° longitude cells.

We projected predictions of the relative environmental suitability for killer whales into geographic space by relating habitat preferences to local conditions using environmental data for different time periods and assuming no changes in species-specific habitat usage over time. For the purpose of this study, we used a slightly modified version of the AQUAMAPS default expert-reviewed envelope settings for killer whales. Specifically, we excluded primary production from the model, as there are no data for Pleistocene conditions including this parameter (Table S7, Supporting information). Comparisons of predictions that excluded (Fig. 1a, present day) or included this parameter (http://www.aquamaps.org/premap.php?map=cached&expert_id=8&SpecID=ITS-180469&cache=1) indicated that model outputs are fairly robust to these changes, resulting only in some localized changes in predicted relative suitability of habitat.

Results

Mitogenome sequences

Complete or nearly complete mitogenome sequences were assembled for 290 samples (283 new, seven resequenced but previously published; Table S1, Supporting information). Haplotypes were assigned sequences with missing data by construction of a neighbour joining tree and comparison to the most similar sequences. We identified 150 unique haplotypes, including previously identified haplotypes from 169 individuals in Morin *et al.* (2010) and Foote *et al.* (2011c, 2013b,c), plus eight sequences with missing data that prevented unambiguous assignment to an existing or unique haplotype. All 158 unique sequences representing 452 individual killer whales (after removal of duplicate sequences from three individuals that were sampled twice; see nuclear SNP analysis below) were used for phylogenetic analysis (Table S1, Supporting information).

Nuclear SNPs

Nuclear locus assemblies and SNP discovery resulted in average depth of coverage of 11.6 and identification of 1605 putative SNPs in a panel of 114 globally distributed samples. From these, 91 SNPs from 42 loci were selected for genotype extraction and analysis (see methods). Multiple SNPs from the same locus were selected based on having different genotype distributions in the sample set (not in phase; Table S3, Supporting information).

A set of 172 samples were genotyped from the sequence data, as not all of the 247 capture-enriched libraries produced sufficient numbers of reads to attempt genotyping from the assembled nuclear sequences. After extraction of SNP genotypes for the selected loci, 130 samples had genotypes from at least 60% of the loci, resulting in data from 128 unique individuals after removal of two samples from individuals that were sampled twice. This threshold was selected to maximize the number of samples while minimizing the impact of missing data on population analyses. Samples were genotyped for an average of 93% of the SNPs (85 of 91 loci), with only 11 of 128 samples having less than 80% (73 of 91 loci) of genotypes completed. The number of samples with sufficiently complete nuclear genotypes ($N = 128$) was, therefore, significantly smaller than for the mitogenome analysis ($N = 452$, including previously published sequences). Genotype data are available from the Dryad repository (doi: 10.5061/dryad.fm4mk).

Analysis of SNPs in three North Pacific populations, the combined North Atlantic strata, and combined Antarctic B and C strata (see methods), indicated that none deviated significantly from expectations of HWE in all five groups, but several deviated significantly in one of the groups and one (GBA_198) deviated significantly in two groups (Table S3, Supporting information). Although between 11 and 56 loci were monomorphic within a group, none were monomorphic across the five groups and only one SNP (ACTC_950) was rare (frequency <0.05) in all five groups. Significant ($P < 0.05$) evidence of LD was found for 2–4 SNPs within eight loci across at least two populations, and an additional three loci when all samples were analysed as a single population. Only two SNP pairs that were not in the same locus showed significant LD across two populations (ELN_554-PIM_839, MATR3_29-TPI1_272). Given this lack of strong evidence for between-locus LD, we used PHASE to combine only SNPs within loci into haplotypes for population analysis. Jackknife analysis for HWE across all samples and within seven ecotype/geographic sample sets did not suggest any sample- or locus-specific genotype issues (such as allelic dropout or null alleles).

Phylogenetic and demographic analyses

The Bayesian maximum-clade-credibility mitogenome phylogeny is presented in Fig. 2. We estimate that the two most divergent lineages of killer whale coalesced about 360 kyr ago (95% CI: 220–530 kyr), with a mean rate of 6.24×10^{-9} (95% CI: 4.27–8.35 $\times 10^{-9}$) substitutions/site/year across the delphinids included in our phylogenetic analysis. Our estimate was based on a secondary calibration for the root of Delphinidae, obtained from an analysis of a multilocus cetacean data set based on multiple fossil calibrations (McGowen *et al.* 2009). The uncertainty in our estimate takes into account the estimation error in the secondary calibration. A spatial component was added to this temporal analysis by inferring the geographic location of ancestral nodes using the BBM method implemented in RASP. Even after setting a conservative threshold of including nodes that we could infer the ancestral geographic location with ≥90% posterior probability, we identified 22 long-range dispersal events with high confidence. It is likely that this under estimates the true number of long-range dispersal events, particularly older events, as the inference of geographic state at ancestral nodes was less certain towards the root of the phylogeny. The phylogenetic pattern of long-range dispersals and the estimated timing of dispersal events are shown in Fig. 3. There was no clear or strong pattern with regard to the timing of dispersal events and the timing of the last glacial maximum, although this was not formally tested and the wide 95% posterior density interval at many nodes make it difficult to assess the precise timing of dispersal relative to climatic events.

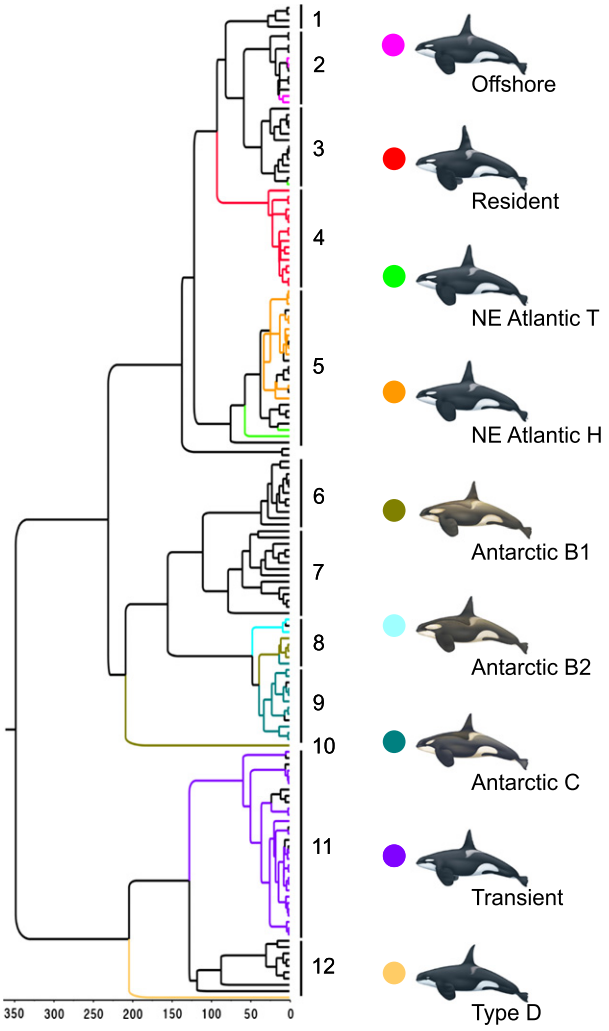

Fig. 2 Bayesian phylogenetic tree of 158 unique mitogenome sequences. Coloured branches identify haplotypes found in individuals identified ecologically or morphologically based on well-characterized types or populations. 'NE Atlantic T' and 'NE Atlantic *H*' represent the herring- and tuna-eating populations, respectively. Solid lines to the right indicate numbered clades referred to in the text. Sample information for haplotypes is provided in Fig. S2 and Table S1 (Supporting information).

SNAPP (Bryant *et al.* 2012) was used to infer phylogenetic relationships from the nuclear loci (Fig. 4). In our data set, all SNPs were polymorphic in multiple populations, and heterozygosity varied strongly among populations, resulting in poor resolution of some clades (posterior <0.5; Fig. 4). Nevertheless, nuclear SNPs clustered the Antarctic B (B1 and B2) and C types into a

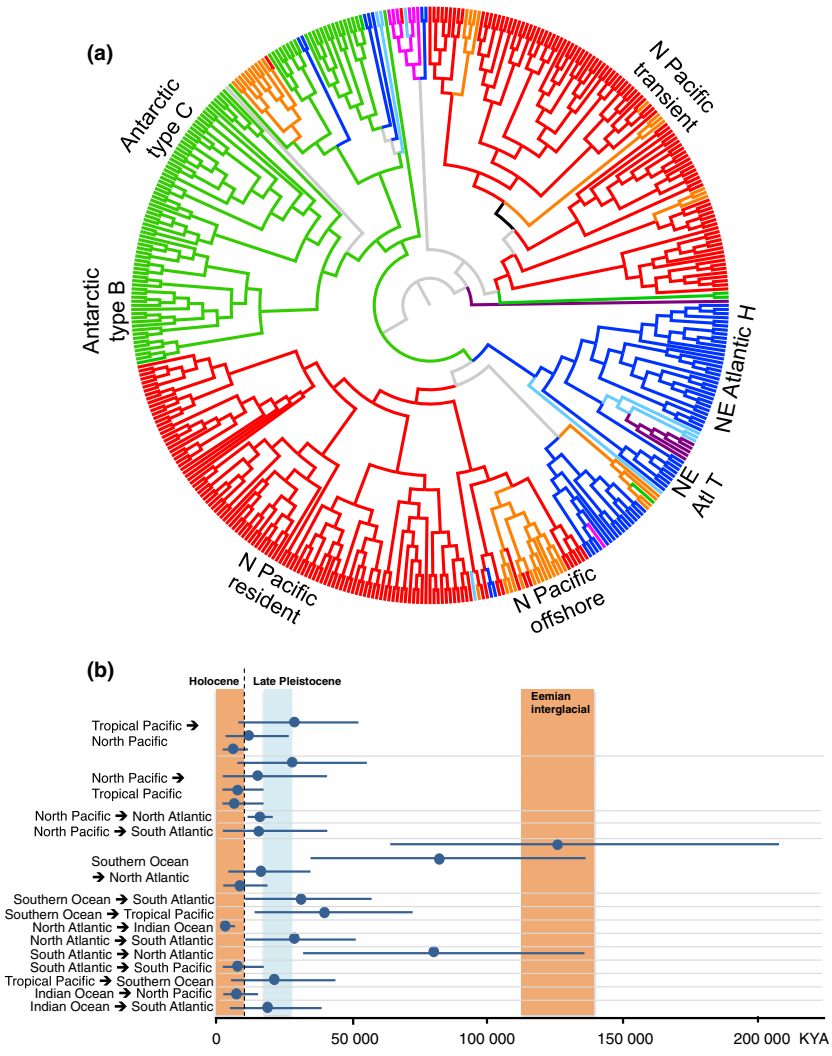

Fig. 3 (a) Circular cladogram showing all samples included in this study. Nodes and branches are coloured based on geographic location (Red = North Pacific; Orange = Tropical Pacific; Purple = South Pacific; Dark Blue = North Atlantic; Light Blue = South Atlantic; Pink = Indian Ocean; Green = Southern Ocean), which for ancestral nodes was inferred using the Bayesian Binary MCMC method implemented in RASP. Only nodes for which geographic location could be inferred at a probability of ≥90% are coloured; nodes with a higher level of uncertainty are unfilled. The estimated timing of predicted dispersal events is shown in (b). Markers show the estimated date of nodes at which the geographic location is inferred to have changed from the ancestral range, when the geographic location for both states is inferred with a posterior probability of ≥90%. Horizontal whiskers show the 95% HPDI of date estimates. Orange bars show the timing of interglacial periods including the current Holocene epoch, and the blue bar indicates the timing of the last glacial maximum.

single clade separate from all others with high probability, and divergent clades for resident, offshore and New Zealand populations. Heterozygosity is preserved in the population model through short time lengths and large population sizes. It may be that the prior on the population sizes is pushing all populations towards a similar N_e, in which case, the branch lengths more closely reflect differences in heterozygosity rather than time, with low-heterozygosity populations being separated from high-heterozygosity populations by longer branches (D. Bryant, personal communication).

In addition to the coalescent model testing in BEAST, we used Tajima's D and Fay and Wu's H tests to look for evidence of population size changes (Table 1). For the species-wide sample set, Tajima's D was positive but not significantly different from zero, indicating no evidence of population size change, although the presence of population structure within the sample set violates assumptions of neutral evolution and may bias the estimates of D (Moeller *et al.* 2007).

We compared the fit of different tree priors and estimated Tajima's D and Fay & Wu's H for a subset of clades (Table 1) to achieve better consistency with the assumption of panmixia and to account for the effect of changes in population size. This included the clades containing the North Pacific resident ecotype and North Atlantic herring-eating population, for which a previous study had inferred a Late Pleistocene demographic decline using the pairwise sequentially Markovian coalescent (PSMC) model applied to a diploid genome of an individual from each clade (Moura *et al.* 2014a). The constant-size model for the coalescent was favoured in the coalescent analysis for each of the four clades. Two clades had excesses of low-frequency polymorphisms, as indicated by a significantly negative Tajima's D (-2.1236, $P < 0.05$) in the Northeast Atlantic clade and a negative value of Tajima's D (-1.468, $P > 0.1$) in the resident clade, consistent with a population expansion following a bottleneck. However, the strongly negative estimate for Fay & Wu's H

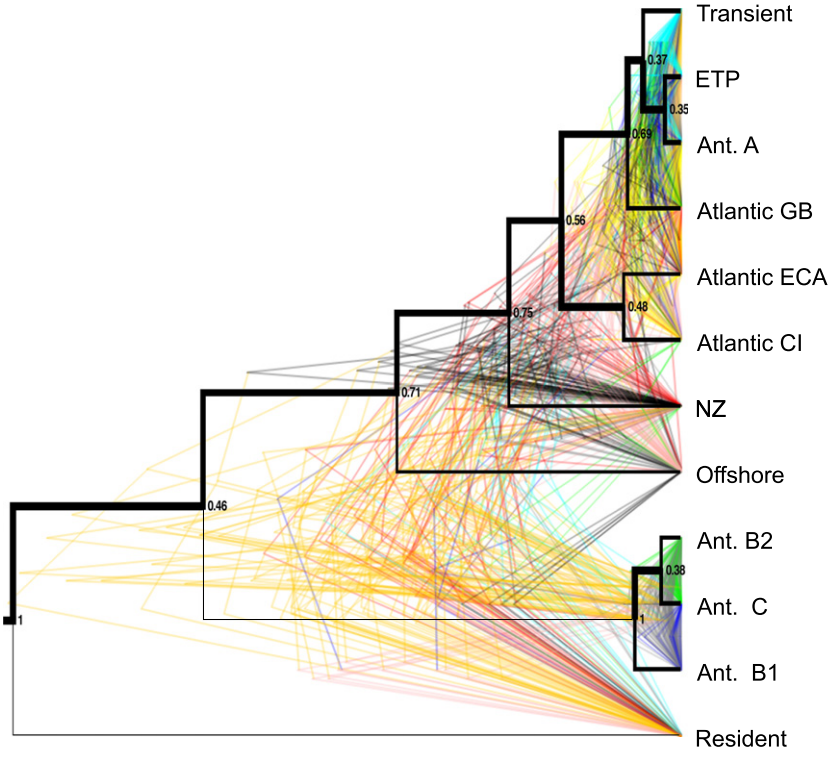

Fig. 4 Nuclear SNP phylogeny based on 42 SNPs. Maximum-clade-credibility tree shown in the black right-angled tree with posterior probabilities at nodes and branch width proportional to theta. Tree cloud of last 50 trees (representing samples taken every 1000 MCMC steps from 50 000 steps) from SNAPP analysis shows the diversity of trees coloured by clade in DENSITREE to make it easier to see the range of topologies. Atlantic populations are as follows: Great Britain (GB), Eastern Canadian Arctic (ECA) and Canary Islands (CI).

Table 1 Estimates of Tajima's *D* and Fay and Wu's *H* (normalized) for all samples and for four clades that correspond to known ecotypes and populations. *N* = number of samples; *S* = number of segregating sites. The outgroup for F&W's *H* test was a transient mitogenome sequence (107847), with the exception of the test for the transient clade, for which a resident mitogenome (126181) was used. The sample group AntC_14774_G are type C killer whales with nonsynonymous substitution in the *cytochrome b* gene, inferred to have evolved under positive selection (Foote *et al.* 2011a)

Sample group	*N*	*S*	Tajima's *D*	Normalized F&W *H*
All_samples	265	174	1.02 ($P > 0.1$)	NA
Antarctic_C	38	20	0.14 ($P > 0.1$)	−1.18
AntC_14774_G	33	11	0.32 ($P > 0.1$)	0.02
Atlantic	32	46	−2.12 ($P < 0.05$)	−2.70
Residents	104	16	−1.47 ($P > 0.1$)	0.43
Transients	91	39	−0.28 ($P > 0.1$)	−0.44

(a statistic insensitive to population expansions) for the Atlantic clade suggests the influence of some previously undetected selection, or more likely, strong population subdivision in our sampling scheme for this clade (e.g. between Iceland and Norway, see Foote *et al.* 2011c), which *H* is highly sensitive to (Zeng *et al.* 2006). There was a strong difference in our estimates of Fay & Wu's *H* for all type C killer whales, compared with just the type C killer whales with a putatively selected mutation at site 14774 (Foote *et al.* 2011a). This statistic is expected to show a dramatic drop in power upon fixation of an advantageous allele (Zeng *et al.* 2006), represented here by the subset including only the specified allele. Comparison of our estimates of Tajima's *D* with Fay and Wu's *H* suggest that the resident clade has an excess of low- but not high-frequency polymorphisms, consistent with a post-bottleneck expansion. However, estimates of both *D* and *H* can be biased by sampling small numbers of individuals from within multiple subpopulations (Zeng *et al.* 2006), which is clearly the case in our sampling of residents from across this ecotype's range (Parsons *et al.* 2013).

Support for populations and ecotypes by nuclear SNPs

For F_{ST} analysis (Table 2), pairwise comparisons of all named ecotypes and morphotypes in the North Pacific and Antarctic were significantly divergent. This is in close agreement with previously published results based on microsatellite genotypes for a subset of these killer whale types (Morin *et al.* 2010; Parsons *et al.* 2013), suggesting that power is similar between these two types of nuclear markers for detecting population differentiation. Significant F_{ST} values indicate little or no gene flow among sympatric ecotypes in the North Pacific (F_{ST} = 0.184–0.433) and Antarctic (F_{ST} = 0.103–0.410).

Habitat model

Our estimated distribution of core suitable habitat during the LGM of 73 million km^2 is smaller than our estimated present-day core suitable habitat distribution of 91 million km^2 (Fig. 1). Similarly, the maximum extent of suitable habitat during the LGM was 300 million km^2 as compared with 350 million km^2 during the present day. With few exceptions, the habitat suitability model corresponds well to the locations of samples included in this study.

Discussion

Our results indicate that killer whales have undergone a rapid global diversification commencing in the Mid-Pleistocene and that long-range dispersal between hemispheres and ocean basins has occurred throughout the Late Pleistocene and Holocene. Long-range dispersers colonized and established new populations, such as around New Zealand, and in some cases mixed with existing lineages, for example in the Eastern Tropical Pacific (ETP). In contrast, other founder lineages remained genetically isolated (resident ecotype) or genetically diversified further following founder events (Antarctic ecotypes), giving rise to the well-characterized ecotypes at high latitudes.

Reconstruction of demographic history with respect to the glacial cycles

We estimate a time to most recent common ancestor (TMRCA) of 0.36 MYA (95% CI: 0.22–0.53 MYA) for all killer whale mitochondrial lineages included in this study. A previous study had estimated the TMRCA at 0.7 MYA (Morin *et al.* 2010), but a subsequent study (Moura *et al.* 2015) argued that this estimate did not account for the time dependence of molecular rates, whereby rate estimates have a negative relationship with the age of the calibration used to obtain them (Ho *et al.* 2011). This pattern, observed in a range of taxonomic groups (e.g. Papadopoulou *et al.* 2010; Duchene *et al.* 2014), is thought to be partly the effect of purifying selection in removing transient mutations over longer time periods (Ho *et al.* 2011). By limiting our analysis to the 3rd codon positions, which are putatively under reduced selection compared with the 1st and 2nd codon positions, we have attempted to account for this problem. The substitution rate for 3rd codon positions was 1.55×10^{-2} substitutions/site/Myr within killer whales (95% CI 0.7×10^{-2}–2.5×10^{-2}) similar to the 3rd codon substitution rate of 2.4×10^{-2} estimated for all cetaceans (Ho & Lanfear 2010). Even taking the 95% credibility interval into consideration,

Table 2 Pairwise F_{ST} (above diagonal) and *P*-values (below diagonal), based on 91 SNPs from 42 loci phased using the samples subdivided by geographic origin or ecotype (strata = 'AS7_PopDiff', Table S4, Supporting information). Sympatric and parapatric groups are boxed in the matrix to highlight divergence among potentially interbreeding populations. Significant *P*-values ($P < 0.05$) are shown in bold. Sample numbers for each population are shown in parentheses. Results from the set of 42 single SNPs are presented in Table S8 (Supporting information)

	Ant_A	Ant_B1	Ant_B2	Ant_C	Crozet	New Zealand	Atl_Canary_Is	Atl_ECA	Atl_GB	ETP	Offshore	Resident	Transient
Ant_A (4)	NA	0.404	0.410	0.334	0.034	0.223	0.080	0.098	0.053	0.026	0.171	0.375	0.021
Ant_B1 (4)	**0.026**	NA	0.141	0.103	0.492	0.504	0.494	0.528	0.578	0.296	0.612	0.676	0.344
Ant_B2 (8)	**0.001**	**0.013**	NA	0.103	0.491	0.515	0.517	0.544	0.566	0.297	0.579	0.635	0.337
Ant_C (7)	**0.004**	**0.004**	**0.004**	NA	0.442	0.451	0.451	0.488	0.507	0.254	0.530	0.613	0.299
Crozet (2)	0.394	0.068	**0.027**	**0.027**	NA	0.296	0.056	0.195	0.104	0.076	0.302	0.465	0.098
New Zealand (4)	**0.023**	**0.035**	**0.001**	**0.004**	0.069	NA	0.017	0.029	0.022	0.002	0.315	0.498	0.247
Atlantic_Canary_Is (4)	0.079	**0.032**	**0.002**	**0.003**	0.204	0.328	NA	0.181	0.141	0.090	0.282	0.443	0.131
Atlantic_ECA (3)	0.081	**0.031**	**0.005**	**0.007**	0.146	0.340	**0.040**	NA	0.112	0.097	0.355	0.397	0.105
Atlantic_GB (3)	0.242	**0.031**	**0.005**	**0.017**	0.239	0.349	**0.025**	0.202	NA	0.098	0.310	0.485	0.137
ETP (24)	0.056	**0.001**	**0.001**	**0.001**	**0.023**	0.177	**0.001**	**0.002**	**0.001**	NA	0.129	0.301	0.045
Offshore (3)	**0.063**	**0.036**	**0.011**	**0.009**	0.100	**0.041**	**0.028**	0.092	0.090	**0.001**	NA	0.433	0.184
Resident (16)	**0.001**	**0.001**	**0.001**	**0.001**	**0.007**	**0.001**	**0.001**	**0.003**	**0.002**	**0.001**	**0.002**	NA	0.283
Transient (30)	0.108	**0.001**	**0.001**	**0.001**	**0.005**	**0.001**	**0.001**	**0.001**	**0.001**	**0.001**	**0.001**	**0.001**	NA

our estimate of the coalescence time differs from those made in previous studies of killer whales. The disparity from the older estimate (Morin *et al.* 2010) might be due to the use of a partitioning strategy in the present analysis, and because sampling was restricted to delphinids. This would have reduced the impact of saturation in our analysis, which can lead to underestimation of the substitution rate. In contrast, our estimated date is older than that of Moura *et al.* (2015) (0.189 MYA), whose estimate was based on nuclear sequence data and a strict clock estimate based on a published substitution rate estimated for cetaceans (no 95% CI reported). It is important to note, however, that this latter TMRCA is for the date at which the sampled recombining nuclear lineages belonged to an interbreeding population, which could have been quite some time after the ancestral nonrecombining mitochondrial lineage gave rise to new daughter lineages.

Our new median date estimate of the initial diversification corresponds with Marine Isotope Stage 11, the warmest and longest interglacial of the last 0.5 MY, with higher sea level and reduced polar ice sheets compared to the present (Howard 1997; Reyes *et al.* 2014); but the 95% CIs overlap with the adjacent glacials. Therefore, the radiation of all sampled extant killer whales from their shared common ancestor to a globally distributed, culturally and morphologically diverse species complex has been a rapid one. It is comparable in geographic and temporal scales with the most recent hominin radiation by *Homo heidelbergensis*, which gave rise to Neanderthals, Denisovans and modern humans (Endicott *et al.* 2010; Prufer *et al.* 2014).

Demographic analysis of the mitochondrial data indicated that the constant-size coalescent model was strongly favoured over models that include changes in population size since the TMRCA. It should be noted that power to infer population history is reduced and coalescent error is increased towards the root of the genealogy, where the population size will be estimated from just two lineages in the oldest coalescent interval (Ho & Shapiro 2011). However, the data suggest that the number of effective females did not go through a global bottleneck during the Late Pleistocene as suggested by Hoelzel *et al.* (2002). Our estimates of Tajima's *D* from individual clades (see Table 1) indicate that some have a deficit and some an excess of low-frequency polymorphisms, suggestive of different processes shaping the demographic history and pattern of genetic diversity within each ecotype/population. The inference of a bottleneck by Hoelzel *et al.* (2002) was largely based upon the site frequency spectrum having an excess of low-frequency polymorphisms, which as noted above could be due to sampling small numbers of individuals from multiple populations (Gattepaille *et al.* 2013).

The lack of support for a demographic bottleneck during the glacial cycles of the Late Pleistocene is consistent with our estimate of just 15% less core suitable habitat being available for killer whales during the LGM compared with the present day (Fig. 1). It is also important to consider, however, that killer whale distributions are largely driven by prey distribution. The range of some prey species with specialized habitat preferences may have been affected by the climatic changes of the LGM and, therefore, could have influenced localized killer whale distribution during the LGM more than predicted by the AquaMaps model. Localized shifts in habitat suitability may also have driven population fragmentation and changes in ice coverage likely influenced interoceanic connectivity, as noted in other marine species (Alter *et al.* 2012, 2015). There was, however, regional release of habitat after the LGM, most notably off the Antarctic continent. A leading edge expansion during this habitat release by the ancestral population of the ecotypes that have colonized the Antarctic pack ice would be expected to be accompanied by a loss of genetic diversity (Hewitt 2000) and would be consistent with the long branch and low estimate of theta in the SNAPP tree.

Current and inferred ancestral biogeography

In contrast to previous mitogenome studies of killer whales, our increased sampling has resulted in almost all clades (including two new clades) consisting of individuals from multiple types, populations and/or diverse geographic locations. Of particular note, killer whales sampled in the Eastern Tropical Pacific (ETP) had haplotypes that fell into clades including North Pacific offshore and transient ecotypes, as well as clustering as sister groups to clades of Southern Ocean and North Atlantic samples. We inferred ancestral dispersal events from high- to lower-latitude populations, with integration of maternal lineages from the transient and offshore ecotype into the lower-latitude ETP population. Our global perspective highlighted a number of cases of relatively recent long-range dispersal events including interoceanic and interhemispheric movement, for example from the North Pacific to the North and South Atlantic, from the Southern Ocean to the Tropical Pacific and North Atlantic, from the North Atlantic to the Indian Ocean (Indonesia) and to New Zealand, and from the Indian Ocean to the North Pacific and South Atlantic.

These inferred examples of long-range dispersal provide potentially important insights into the evolution of sympatric ecotypes found in some locations. We found the BBM method implemented in RASP had insufficient power to robustly infer ancestral distributions close to

the root of the phylogeny. This was particularly evident in cases of rapid successive divergences, which included the nodes that have been previously used to infer phylogeographic patterns and assess the case for sympatric diversification vs. secondary contact among North Pacific ecotypes (see Foote *et al.* 2011b; Foote & Morin 2015; Moura *et al.* 2015). However, in other cases, we find sympatry of very divergent and presumably previously allopatric mitochondrial lineages. For example, two individuals that stranded on the west coast of Scotland in the past decade, which Foote *et al.* (2009) had assigned to a local type (type 2, which differed in isotopic signature and tooth wear from the more common type 1 Northeast Atlantic samples), were nested in a clade containing Southern Ocean killer whales (clade 7). There were several such strongly supported cases of long-range dispersal bringing highly diverged matrilineal lineages into secondary contact.

The mitochondrial genome is only a single locus and therefore represents a single reconstruction of a highly stochastic process (the coalescent), and due to its strict maternal inheritance tracks only the matrilineal population history. Therefore, analyses of the mitochondrial genome are expected to have less power to detect ancestral demographic change than analyses of multiple nuclear loci (Heled & Drummond 2008). The extent to which we can reliably infer the evolutionary history of the radiation and diversification of killer whales from our mitogenome data depends upon whether this single-locus tree reflects the true population history. Phylogeographic analysis of mitochondrial DNA trees can, under certain scenarios, be a powerful tool for population genetic analysis (Zink & Barrowclough 2008). If migration and founding events are associated with population bottlenecks when a small number of individuals colonizes new territory and then remains largely reproductively isolated from other local populations (the process proposed for establishment of discrete killer whale populations in Foote *et al.* 2011b,c; Hoelzel *et al.* 2007, 2002; Morin *et al.* 2010), then the newly established populations will be monophyletic and (nuclear and mitochondrial) lineages will coalesce back to this founding event. Under such a scenario, single gene trees can provide a useful insight into population history and phylogeography (Nielsen & Beaumont 2009). The nuclear data presented here (Fig. 4) and in another recently published study (Moura *et al.* 2015) suggest that nuclear and mitochondrial phylogenies are to some extent concordant and that most of the well-characterized ecotypes cluster in monophyletic nuclear clades (although the relationship between clades may differ between nu and mt trees; see Moura *et al.* 2015). However, in cases of multiple rapid population splits, mitochondrial introgression (see below) or gene flow upon secondary contact, the branching order may not accurately reconstruct the chronology of this radiation.

The nuclear phylogeny presented here (Fig. 4) is less well resolved than the mitochondrial phylogeny despite significant divergence metrics suggesting low to zero levels of contemporary gene flow between ecotypes (Table 2). Lineage sorting is expected to be faster for mitochondrial than nuclear DNA because of differences in effective population size (Avise 1989). The difference in lineage sorting rates is likely to be inflated in killer whales based on the observed pattern of limited or no dispersal from the natal population, but some male-mediated gene flow among populations (Hoelzel *et al.* 2007). It is not surprising, therefore, that all of our nuclear SNPs are polymorphic in multiple populations and do not show the corresponding patterns of fixed private mutations in any of our killer whale populations. However, as noted above, we do see evidence for founder effects in the nuclear phylogeny produced by SNAPP potentially having a role in the rapid lineage sorting in some of well-characterized ecotypes. We estimate relatively low effective population size (θ) along the branches leading to the resident and to the ancestral node of the Antarctic types B1, B2 and C (Fig. 4). SNAPP infers θ values using a Bayesian coalescent analysis. However, the small number (42) of SNPs can make θ estimates unreliable, both due to the variability of the posterior distribution and the increased impact of the prior (Bryant *et al.* 2012; D. Bryant, personal communication).

We do find some cases where the mitochondrial tree may not reflect the true population history. For example, all mitochondrial and nuclear DNA phylogenies to date are incongruent for the placement of the offshore ecotype (Barrett-Lennard 2000; Foote & Morin 2015; Moura *et al.* 2015; Pilot *et al.* 2010; this study). A second example is the Antarctic type B morphotype, which was monophyletic in our previous study but here included an individual assigned as type B based on phenotype and nuclear markers, but which had a unique and highly divergent mitochondrial DNA haplotype (ANTB6). These mito-nuclear incongruences probably reflect a combination of incomplete lineage sorting and/or more recent introgression between divergent lineages. Nevertheless, the distinctiveness (monophyly) and inferences of unique founding events in the mtDNA tree are consistent with the previous studies for all ecotypes and morphotypes. Of particular note are the monophyly (despite significantly larger sample sizes) of the North Pacific residents and Antarctic type C killer whales, and inclusion of all North Pacific transient and offshore ecotype samples within their respective clades with no shared haplotypes among these types. These results continue to support the genetic

cohesiveness of several of the named ecotypes, with origins of the ancestral lineages dating from ~50 000 to 350 000 years ago (Fig. 2). Ultimately, the resolution obtained by sequencing large numbers of nuclear loci (e.g. Moura *et al.* 2015) and comprehensive taxon sampling (such as in this study) is needed to fully elucidate the population history of killer whales at a global scale.

In summary, by sampling globally and using a relatively fast-evolving marker (mtDNA), we highlight how a rapid (~10 000 generations) ecological and geographic radiation can result in a rapid build-up of genetic differentiation and lineage sorting, even in species with a long generation time and a relatively slow molecular clock. Arguably, the most interesting aspect of killer whale biology is their propensity for ecological diversification and for reproductive isolation barriers to quickly form between ecotypes and be maintained even in sympatry. By sampling globally, we have highlighted the frequency at which geographic regions are colonized by secondary invasion resulting in sympatry between divergent killer whale lineages that had previously existed in allopatry. As noted earlier, in threespine stickleback, such post-glacial double invasions have resulted in character displacement and the evolution of two different forms. Our study thereby sets the stage for further investigation as to whether this is a key mechanism underlying the evolution of reproductively isolated killer whale ecotypes.

Acknowledgements

We are grateful to the following people and organizations for providing valuable samples that contributed towards both the new sequences produced here and the previously generated and published sequences that this new work builds upon: Southwest Fisheries Science Center Marine Mammal and Turtle Molecular Research Sample Collection and SWFSC researchers who collected samples; Katja Vinding Petersen and Henrik Egede-lassen, Natural History Museum of Denmark; Natural History Museum, London; Scottish Agricultural College; Scott Baker and the New Zealand Cetacean Tissue Archive curated at the University of Auckland; The New Zealand Department of Conservation (DOC); Charles Potter and the US National Museum of Natural History (Accession nos 238112, 238119, 241401, 550857, 571360); Robin Baird, Greg Schorr and the Cascadia Research Collective; Ken Balcomb; Jorge Urban; Erin Oleson; Instituto Aqualie; Natalie Goodall; the Hawaii Pacific University Stranding Program; Brad Hanson and Candice Emmons (Northwest Fisheries Science Center); Vladimir Burkanov; Alexander Burdin; Gisli Vikingsson, MRI, Reykjavik; Nils Øien, IMR, Bergen; Renaud de Stephanis and Philippe Verborgh, CIRCE; Bob Reid, Scottish Agricultural College; and the International Whaling Commission. All samples were collected under appropriate permits (MMPA in the U.S.) and transferred to the SWFSC under CITES permit if shipped internationally. Funding was provided by the Alaska Fisheries Science Center, the Northwest Fisheries Science Center, the National Marine Fisheries Service Office of Science and Technology, Fisheries and Oceans Canada, the Marie Curie Actions (KWAF2010) and the Danish Basic Research Foundation (DNRF94). We are thankful to Steve Head and the staff at The Scripps Research Institute Microarray Core, and Gerald Pao and Manching Ku, Salk Institute for Biological Studies, for sequencing assistance. Uko Gorter kindly provided his images of killer whale ecotypes, and Béla Dornon assisted with graphics. The manuscript was significantly improved through thoughtful review by Bob Pitman, Bill Perrin, Barbara Taylor, Tim Vines and three anonymous reviewers from Axios Review, and three other anonymous reviewers.

References

Alter SE, Rosenbaum HC, Postma LD *et al.* (2012) Gene flow on ice: the role of sea ice and whaling in shaping Holarctic genetic diversity and population differentiation in bowhead whales (*Balaena mysticetus*). *Ecology and Evolution*, **2**, 2895–2911.

Alter SE, Meyer M, Post K *et al.* (2015) Climate impacts on transocean dispersal and habitat in gray whales from the Pleistocene to 2100. *Molecular Ecology*, **24**, 1510–1522.

Amaral AR, Beheregaray LB, Bilgmann K *et al.* (2012) Influences of past climatic changes on historical population structure and demography of a cosmopolitan marine predator, the common dolphin (genus *Delphinus*). *Molecular Ecology*, **21**, 4854–4871.

Avise JC (1989) Gene trees and organismal histories – a phylogenetic approach to population biology. *Evolution*, **43**, 1192–1208.

Barrett-Lennard LG (2000) *Population structure and mating patterns of killer whales (Orcinus orca) as revealed by DNA analysis*. Ph.D. Thesis, Univ. British Columbia, Vancouver, BC.

Bigg MA, Olesiuk GM, Ellis GM, Ford JKB, Balcomb KC (1990) Social organization and genealogy of resident killer whales (*Orcinus orca*) in the coastal waters of British Columbia and Washington State. *Report to the International Whaling Commission (Special Issue)*, **12**, 386–406.

Blois JL, McGuire JL, Hadly EA (2010) Small mammal diversity loss in response to late-Pleistocene climatic change. *Nature*, **465**, 771–774.

Bouckaert RR (2010) DensiTree: making sense of sets of phylogenetic trees. *Bioinformatics*, **26**, 1372–1373.

Bryant D, Bouckaert R, Felsenstein J, Rosenberg NA, RoyChoudhury A (2012) Inferring species trees directly from biallelic genetic markers: bypassing gene trees in a full coalescent analysis. *Molecular Biology & Evolution*, **29**, 1917–1932.

Carstens BC, Knowles LL (2007) Shifting distributions and speciation: species divergence during rapid climate change. *Molecular Ecology*, **16**, 619–627.

Carto SL, Weaver AJ, Hetherington R, Lam Y, Wiebe EC (2009) Out of Africa and into an ice age: on the role of global climate change in the late Pleistocene migration of early modern humans out of Africa. *Journal of Human Evolution*, **56**, 139–151.

Drummond AJ, Rambaut A (2007) BEAST: Bayesian evolutionary analysis by sampling trees. *BMC Evolutionary Biology*, **7**, 214.

Drummond AJ, Ho SY, Phillips MJ, Rambaut A (2006) Relaxed phylogenetics and dating with confidence. *PLoS Biology*, **4**, e88.

Drummond AJ, Suchard MA, Xie D, Rambaut A (2012) Bayesian phylogenetics with BEAUti and the BEAST 1.7. *Molecular Biology & Evolution*, **29**, 1969–1973.

Duchene S, Holmes EC, Ho SY (2014) Analyses of evolutionary dynamics in viruses are hindered by a time-dependent bias in rate estimates. *Proceedings of the Royal Society of London, B*, **281**, 20140732.

Endicott P, Ho SY, Stringer C (2010) Using genetic evidence to evaluate four palaeoanthropological hypotheses for the timing of Neanderthal and modern human origins. *Journal of Human Evolution*, **59**, 87–95.

Fay JC, Wu CI (2000) Hitchhiking under positive Darwinian selection. *Genetics*, **155**, 1405–1413.

Flicek P, Ahmed I, Amode MR *et al.* (2013) Ensembl 2013. *Nucleic Acids Research*, **41**, D48–D55.

Foote AD, Morin PA (2015) Sympatric speciation in killer whales? *Heredity*, **114**, 537–538.

Foote AD, Newton J, Piertney SB, Willerslev E, Gilbert MTP (2009) Ecological, morphological and genetic divergence of sympatric North Atlantic killer whale populations. *Molecular Ecology*, **18**, 5207–5217.

Foote AD, Morin PA, Durban JW *et al.* (2011a) Positive selection on the killer whale mitogenome. *Biology Letters*, **7**, 116–118.

Foote AD, Morin PA, Durban JW *et al.* (2011b) Out of the Pacific and back again: insights into the matrilineal history of Pacific killer whale ecotypes. *PLoS ONE*, **6**, e24980.

Foote AD, Vilstrup JT, De Stephanis R *et al.* (2011c) Genetic differentiation among North Atlantic killer whale populations. *Molecular Ecology*, **20**, 629–641.

Foote AD, Kaschner K, Schultze SE *et al.* (2013a) Ancient DNA reveals that bowhead whale lineages survived Late Pleistocene climate change and habitat shifts. *Nature Communications*, **4**, 1677.

Foote AD, Morin PA, Pitman RL *et al.* (2013b) Mitogenomic insights into a recently described and rarely observed killer whale morphotype. *Polar Biology*, **36**, 1519–1523.

Foote AD, Newton J, Avila-Arcos MC *et al.* (2013c) Tracking niche variation over millennial timescales in sympatric killer whale lineages. *Proceedings of the Royal Society of London, B*, **280**, 20131481.

Ford JKB, Ellis GM, Barrett-Lennard LG *et al.* (1998) Dietary specialization in two sympatric populations of killer whales (*Orcinus orca*) in coastal British Columbia and adjacent waters. *Canadian Journal of Zoology*, **76**, 1456–1471.

Ford JKB, Ellis GM, Balcomb KCI (2000) *Killer Whales: The Natural History and Genealogy of Orcinus orca in British Columbia and Washington State*, 2nd edn. University of British Columbia Press, Vancouver.

Ford JKB, Ellis GM, Matkin CO *et al.* (2011) Shark predation and tooth wear in a population of northeastern Pacific killer whales. *Aquatic Biology*, **11**, 213–224.

Forney KA, Wade PR (2006) Worldwide distribution and abundance of killer whales. In: *Whales, Whaling and Ocean Ecosystems* (eds Estes JA, DeMaster DP, Doak DF, Williams TM, Brownell RL Jr), pp. 145–162. University of California Press, Berkeley, California.

Gattepaille LM, Jakobsson M, Blum MG (2013) Inferring population size changes with sequence and SNP data: lessons from human bottlenecks. *Heredity*, **110**, 409–419.

Hancock-Hanser B, Frey A, Leslie M *et al.* (2013) Targeted multiplex next-generation sequencing: advances in techniques of mitochondrial and nuclear DNA sequencing for population genomics. *Molecular Ecology Resources*, **13**, 254–268.

Heled J, Drummond AJ (2008) Bayesian inference of population size history from multiple loci. *BMC Evolutionary Biology*, **8**, 289.

Hewitt GM (1996) Some genetic consequences of ice ages, and their role in divergence and speciation. *Biological Journal of the Linnean Society*, **58**, 247–276.

Hewitt G (2000) The genetic legacy of the Quaternary ice ages. *Nature*, **405**, 907–913.

Ho SY, Lanfear R (2010) Improved characterisation of among-lineage rate variation in cetacean mitogenomes using codon-partitioned relaxed clocks. *Mitochondrial DNA*, **21**, 138–146.

Ho SY, Shapiro B (2011) Skyline-plot methods for estimating demographic history from nucleotide sequences. *Molecular Ecology Resources*, **11**, 423–434.

Ho SY, Lanfear R, Bromham L *et al.* (2011) Time-dependent rates of molecular evolution. *Molecular Ecology*, **20**, 3087–3101.

Hoelzel AR, Natoli A, Dahlheim ME *et al.* (2002) Low worldwide genetic diversity in the killer whale (*Orcinus orca*): implications for demographic history. *Proceedings of the Royal Society of London, B*, **269**, 1467–1473.

Hoelzel AR, Hey J, Dahlheim ME *et al.* (2007) Evolution of population structure in a highly social top predator, the killer whale. *Molecular Biology & Evolution*, **24**, 1407–1415.

Hofreiter M, Barnes I (2010) Diversity lost: are all Holarctic large mammal species just relict populations? *BMC Biology*, **8**, 46.

Howard WR (1997) Palaeoclimatology – A warm future in the past. *Nature*, **388**, 418–419.

Kaschner K, Tittensor DP, Ready J, Gerrodette T, Worm B (2011) Current and future patterns of global marine mammal biodiversity. *PLoS ONE*, **6**, e19653.

Lanfear R, Calcott B, Ho SY, Guindon S (2012) Partitionfinder: combined selection of partitioning schemes and substitution models for phylogenetic analyses. *Molecular Biology & Evolution*, **29**, 1695–1701.

Librado P, Rozas J (2009) DnaSP v5: a software for comprehensive analysis of DNA polymorphism data. *Bioinformatics*, **25**, 1451–1452.

Lindblad-Toh K, Garber M, Zuk O *et al.* (2011) A high-resolution map of human evolutionary constraint using 29 mammals. *Nature*, **478**, 476–482.

Lorenzen ED, Nogues-Bravo D, Orlando L *et al.* (2011) Species-specific responses of Late Quaternary megafauna to climate and humans. *Nature*, **479**, 359–364.

Lovette IJ (2005) Glacial cycles and the tempo of avian speciation. *Trends in Ecology & Evolution*, **20**, 57–59.

McGowen MR, Spaulding M, Gatesy J (2009) Divergence date estimation and a comprehensive molecular tree of extant cetaceans. *Molecular Phylogenetics and Evolution*, **53**, 891–906.

McKinnon JS, Rundle HD (2002) Speciation in nature: the threespine stickleback model systems. *Trends in Ecology & Evolution*, **17**, 480–488.

Moeller DA, Tenaillon MI, Tiffin P (2007) Population structure and its effects on patterns of nucleotide polymor-

phism in teosinte (*Zea mays* ssp. *parviglumis*). *Genetics*, **176**, 1799–1809.

Morin PA, LeDuc RG, Robertson KM *et al.* (2006) Genetic analysis of killer whale (*Orcinus orca*) historical bone and tooth samples to identify western U.S. ecotypes. *Marine Mammal Science*, **22**, 897–909.

Morin PA, LeDuc RG, Archer FI *et al.* (2009) Significant deviations from Hardy–Weinberg equilibrium caused by low levels of microsatellite genotyping errors. *Molecular Ecology Resources*, **9**, 498–504.

Morin PA, Archer FI, Foote AD *et al.* (2010) Complete mitochondrial genome phylogeographic analysis of killer whales (*Orcinus orca*) indicates multiple species. *Genome Research*, **20**, 908–916.

Moura AE, Janse van Rensburg C, Pilot M *et al.* (2014a) Killer whale nuclear genome and mtDNA reveal widespread population bottleneck during the last glacial maximum. *Molecular Biology & Evolution*, **31**, 1121–1131.

Moura AE, Kenny JG, Chaudhuri R *et al.* (2014b) Population genomics of the killer whale indicates ecotype evolution in sympatry involving both selection and drift. *Molecular Ecology*, **23**, 5179–5192.

Moura AE, Kenny JG, Chaudhuri RR *et al.* (2015) Phylogenomics of the killer whale indicates ecotype divergence in sympatry. *Heredity*, **114**, 48–55.

Muller UC, Pross J, Tzedakis PC *et al.* (2011) The role of climate in the spread of modern humans into Europe. *Quaternary Science Reviews*, **30**, 273–279.

Nielsen R, Beaumont MA (2009) Statistical inferences in phylogeography. *Molecular Ecology*, **18**, 1034–1047.

O'Corry-Crowe G (2008) Climate change and the molecular ecology of Arctic marine mammals. *Ecological Applications*, **18**, S56–S76.

Papadopoulou A, Anastasiou I, Vogler AP (2010) Revisiting the insect mitochondrial molecular clock: the mid-aegean trench calibration. *Molecular Biology and Evolution*, **27**, 1659–1672.

Parsons KM, Durban JW, Burdin AM *et al.* (2013) Ecological specialization and the genetic structuring of killer whale populations in the far North Pacific. *Molecular Ecology*, **104**, 737–754.

Pastene LA, Goto M, Kanda N *et al.* (2007) Radiation and speciation of pelagic organisms during periods of global warming: the case of the common minke whale, *Balaenoptera acutorostrata*. *Molecular Ecology*, **16**, 1481–1495.

Pilot M, Dahlheim ME, Hoelzel AR (2010) Social cohesion among kin, gene flow without dispersal and the evolution of population genetic structure in the killer whale (*Orcinus orca*). *Journal of Evolutionary Biology*, **23**, 20–31.

Pitman RL, Ensor P (2003) Three forms of killer whales (*Orcinus orca*) in Antarctic waters. *Journal of Cetacean Research and Management*, **5**, 131–139.

Prufer K, Racimo F, Patterson N *et al.* (2014) The complete genome sequence of a Neanderthal from the Altai Mountains. *Nature*, **505**, 43–49.

R Development Core Team (2011) *R: A Language and Environment for Statistical Computing*. R Foundation for Statistical Computing, Vienna, Austria.

Raymond M, Rousset F (1995) GENEPOP (version 1.2): population genetics software for exact tests and ecumenicism. *Journal of Heredity*, **86**, 248–249.

Ready J, Kaschner K, South AB *et al.* (2010) Predicting the distributions of marine organisms at the global scale. *Ecological Modelling*, **221**, 467–478.

Reyes AV, Carlson AE, Beard BL *et al.* (2014) South Greenland ice-sheet collapse during Marine Isotope Stage 11. *Nature*, **510**, 525–528.

Ronquist F (2004) Bayesian inference of character evolution. *Trends in Ecology & Evolution*, **19**, 475–481.

Stephens M, Smith NJ, Donnelly P (2001) A new statistical method for haplotype reconstruction from population data. *American Journal of Human Genetics*, **68**, 978–989.

Sturmbauer C, Baric S, Salzburger W, Ruber L, Verheyen E (2001) Lake level fluctuations synchronize genetic divergences of cichlid fishes in African lakes. *Molecular Biology and Evolution*, **18**, 144–154.

Tajima F (1989) Statistical method for testing the neutral mutation hypothesis by DNA polymorphism. *Genetics*, **123**, 585–595.

Wagner CE, Keller I, Wittwer S *et al.* (2013) Genome-wide RAD sequence data provide unprecedented resolution of species boundaries and relationships in the Lake Victoria cichlid adaptive radiation. *Molecular Ecology*, **22**, 787–798.

Weir BS, Cockerham CC (1984) Estimating F-Statistics for the Analysis of Population-Structure. *Evolution*, **38**, 1358–1370.

Wright S (1931) Evolution in Mendelian Populations. *Genetics*, **16**, 97–159.

Yu Y, Harris AJ, He X-J (2014) RASP (Reconstruct Ancestral State in Phylogenies) 3.0. Available at http://mnh.scu.edu.cn/soft/blog/RASP

Zeng K, Fu YX, Shi S, Wu CI (2006) Statistical tests for detecting positive selection by utilizing high-frequency variants. *Genetics*, **174**, 1431–1439.

Zink RM, Barrowclough GF (2008) Mitochondrial DNA under siege in avian phylogeography. *Molecular Ecology*, **17**, 2107–2121.

P.A.M., A.D.F., K.M.P., K.K., P.R.W., J.W.D., J.K.F., M.J.F. and M.T.P.G. were involved in design of the research; P.A.M., A.D.F., S.Y.W.H., K.K. and K.M.R. performed the research and analysed the data; F.I.A., M.C.Á.-A. and C.G. provided analytical tools; L.G.B.-L., C.O.M., G.M.E., S.D.P., S.H.F., I.N.V. and L.D.R. provided samples and collection data; P.A.M. and A.D.F. wrote the manuscript.

Data accessibility

DNA sequences: GenBank Accession nos KR180297–KR180367 (mitochondrial haplotypes), KR014267–KR014271 (nuclear sequences).

SNP genotypes: doi: 10.5061/dryad.fm4mk.

BEAST input XML file and maximum-clade-credibility output tree file for aligned mitogenome haplotypes: Dryad doi: 10.5061/dryad.fm4mk.

SNAPP input and output files for SNP phylogenetic analysis: Dryad doi: 10.5061/dryad.fm4mk.

Supporting information

Additional supporting information may be found in the online version of this article.

Fig. S1 Results from 128 killer whale samples and 91 SNPs analyzed with the program STRUCTURE.

Fig. S2 This figure is the same as Figure 2 in the main text, but with sample names that indicate the haplotype ID and abbreviated geographic locations where the haplotype was found.

Table S1 Sample and mitogenome sequencing information.

Table S2 Summary of nuclear sequences used for capture array.

Table S3 (A) Individual SNP data from all samples. Calculated values were obtained using the "summarize.loci" function the R package StrataG. (B) Summary of average values for 5 strata, 91 SNPs. (C) Methods for SNP validation.

Table S4 Strata used to generate multi-SNP genotypes with PHASE (populations in "AS7_All_Pops") and for population analyses with STRUCTURE and divergence metrics (F_{ST}).

Table S5 Delphinidae mitogenome sequences used in phylogenetic analysis.

Table S6 Partitioning schemes and mutation models used for BEAST analyses.

Table S7 Envelope settings used for generating AquaMaps predictions.

Table S8 Pairwise F_{ST} values for population comparisons with 91 phased SNPs and with 42 individual SNPs.